



# ASSESSMENT OF MULTIDIRECTIONAL STIFFNESS OF A UNIFORMLY GRADED GRAVEL USING DISK TRANSDUCERS

Troyee Tanu DUTTA<sup>1</sup>, Masahide OTSUBO<sup>2</sup>,  
Reiko KUWANO<sup>3</sup> and Takeshi SATO<sup>4</sup>

**ABSTRACT:** The utilization of gravelly materials in various geotechnical applications, necessitates the accurate estimation of small strain stiffness to describe their stability and deformation characteristics. Granular materials are observed to be inherently anisotropic in nature displaying dissimilar stiffness in vertical and horizontal directions during deposition of the particles or during compaction. In the present study, a new design configuration of planar piezoelectric transducers is proposed which can assess nine different stiffnesses to describe the stiffness anisotropy of granular material. It is seen that stiffness measured in horizontal directions are considerably greater than those calculated in the vertical direction

**Key Words:** *Disk transducers, shear moduli, Young's moduli, inherent anisotropy, gravel*

## INTRODUCTION

The assessment of stiffness behavior of soils at small strain level is essential for the design of numerous geotechnical structures. The utilization of gravelly materials in numerous geotechnical applications, such as embankments, dams, tunnels, railways, roads etc., necessitates the accurate estimation of small strain stiffness to describe their stability and deformation characteristics. Nevertheless, the research focusing on the determination of small strain stiffness of gravels are somewhat limited (Kokusho and Yoshida 1997; Modoni et al., 2000; AnhDan et al., 2002 and Dutta et al. 2019).

The use of piezoelectric transducers for the measurement of small strain stiffness was pioneered by Lawrence (1965) and Shirley and Hampton (1978), who developed the ubiquitously used bender elements to perform wave velocity measurements. These types of transducers perform on the principle of piezoelectricity where applied excitation voltage is converted to pressure and vice versa. The bender element technique is not suitable for the wave velocity measurement of coarse-grained soils (such as coarse sands and gravels), undisturbed and cemented soils. Hence, the previous researchers started adopting planar piezoelectric transducers also known as disk transducers (Brignoli et al. 1996; Ismail and Rammah, 2005; Suwal and Kuwano, 2013; Otsubo and O'Sullivan 2018). However, there is a paucity of research conducted on the development and adoption of planar piezoelectric transducers for wave velocity measurements of gravels (Dutta et al. 2019).

Granular materials are observed to be inherently anisotropic in nature exhibiting dissimilar stiffness in

---

<sup>1</sup> Doctoral student, Department of Civil Engineering, The University of Tokyo

<sup>2</sup> Research Associate, Institute of Industrial Science, The University of Tokyo

<sup>3</sup> Professor, Institute of Industrial Science, The University of Tokyo

<sup>4</sup> Technical Director, Integrated Geotechnology Institute Limited

vertical and horizontal directions during the process of deposition of the particles or during compaction (Hoque and Tatsuoka, 1998). A myriad of researchers started installing an assembly of vertical and horizontal bender elements (Pennington et al., 1997; Kuwano and Jardine, 2002; Santamarina and Cho, 2004; Ng and Yung, 2008; Wang and Mok, 2008; Escribano and Nash, 2015) to illustrate the inherent anisotropic behavior of soils. Moreover, research has been also undertaken on true triaxial test apparatus by means of applying small amplitude cyclic loadings in both vertical and horizontal directions to quantify the inherent anisotropy of soils (Hoque and Tatsuoka, 1998, Jiang et al., 1997, AnhDan et al., 2002).

In the current study, the development of a novel test setup which employs disk transducers for the measurement of vertical and horizontal stiffness to quantify stiffness anisotropy has been described. The disk transducers were installed in a large triaxial apparatus having rectangular specimen of dimension 236×236×500 mm and hence, this device is capable of measuring wave velocities ( $V_s$  and  $V_p$ ) of soils having a wide range of mean particle sizes ( $D_{50}$ ) (from fine sands to gravels). The wave velocity measurements were performed on a uniformly graded gravel and discussions on the time domain responses and stiffness anisotropy are made.

## MATERIAL PROPERTY

The material tested in the present study is Oiso gravel which is uniformly graded, greyish color, relatively round, elongated shaped gravel acquired from Oiso town of Kanagawa Prefecture of Japan (Figure 1). The grain size distribution curve of the Oiso gravel shows a median particle size ( $D_{50}$ ) of 11.8 mm (Figure 2). The specific gravity ( $G_s$ ) and uniformity coefficient ( $U_c$ ) of Oiso gravel are 2.57 and 1.22, respectively. The maximum ( $e_{max}$ ) and minimum ( $e_{min}$ ) void ratios are 0.624 and 0.480 respectively.



**Figure 1** Picture of Oiso gravel

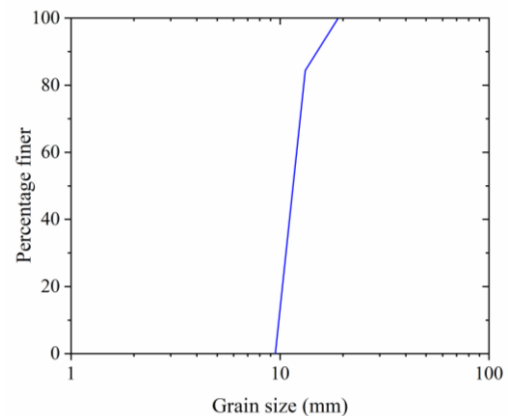


**Figure 2** Grain size distribution

## DEVELOPMENT OF DISK TRANSDUCERS

### *Vertical Disk Transducers*

The piezoelectric disks comprising of P and S plates are of the dimension 20 mm in diameter and 2 mm thick and are factory manufactured by Fuji Ceramic Corporation (Fig. 2). The chemical composition of the piezoelectric material is Lead Zirconate Titanate Ceramic [ $Pb(Ti.Zr)O_3$ ]. The polarization of the P disks is perpendicular to the electrodes and on the other hand, S plates are polarized in parallel direction to the electrodes (Suwal and Kuwano, 2013).

For the vertical disk transducer, a stainless-steel disk of 80 mm diameter performs as a single unit and for each transmitter and receiver assembly, eight numbers of S- plates and four numbers of P- plates were used. Taking the sample length of 500 mm into account, for each layer of S- and P- plates, a circular array of four disks were used to increase the amplitude of the signal. An SSP- arrangement of piezoelectric transducer is created by merging two layers of S- plates oscillating in mutually

perpendicular directions and one layer of P- plates (as displayed in Figure 3). In between each of the layers of SSP- assembly, acrylic plates of thickness 1 mm are placed to separate the piezoelectric disks. The P- plates of the SSP- arrangement are attached to an acrylic plate and are placed farther from the specimen. The acrylic plate adjacent to the P plate- is screwed to a stainless-steel disk of diameter 86 mm. Subsequently, the top S- disks were attached to a 1 mm thick acrylic plate and screwed to another 80 mm diameter stainless steel plate. Figure 4 presents the developed transmitter element for performing wave measurement and by repeating the above-mentioned steps a receiver element is designed.

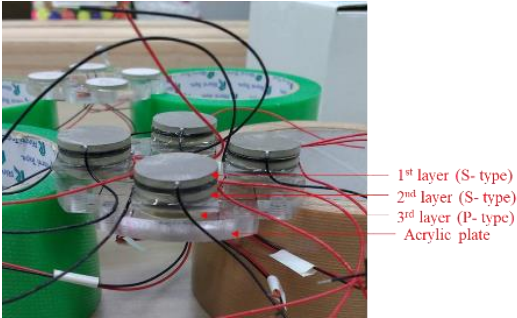


**Figure 3** SSP- arrangement of disk transducer

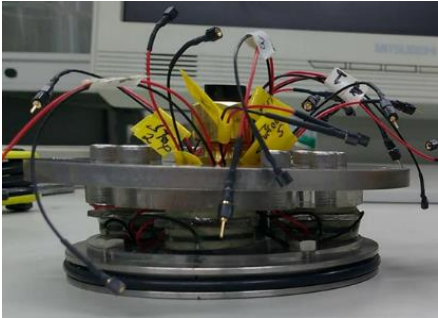


**Figure 4** Transmitter element

Due to complex design of the transmitter and receiver assembly, calibration exercise is performed initially by directly attaching both the faces of the transmitter and receiver element (Figure 5). The excitation wave signals were produced using a digital function generator which was then amplified by a bipolar amplifier ( $\pm 70V$ ). The amplified input signal was sent to the transmitter element of the disk transducer. Figure 6 demonstrates the time domain responses for different layers of piezoelectric transducers during direct contact of transmitter and receiver elements. It can be visualized that all the three layers (SSP-) of piezoelectric disks exhibit negligible time lag, but the P disks located at the rear end show lower output amplitude as compared to the S- layers.

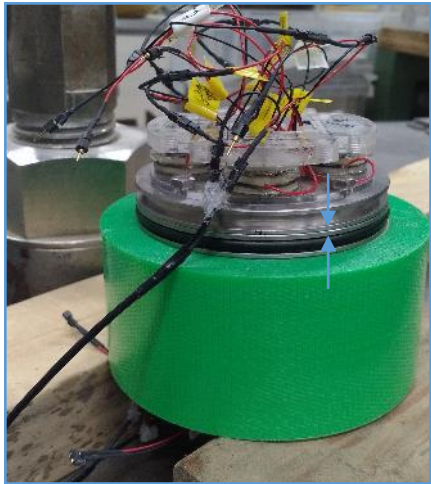


**Figure 5** Calibration of vertical disk transducers

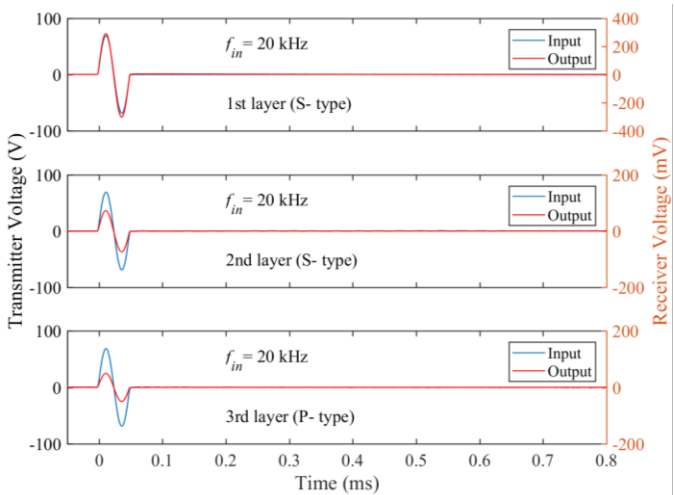


**Figure 6** Time domain response during calibration

The transmitter assembly is provided a parallel connection to generate an equal input voltage to all the transmitting elements, whereas series connection was given for the receiver elements to gain maximum output voltage. The transmitter is fastened to a rectangular stainless-steel plate using screws which is fixed to the top cap, while the receiver is attached directly to the bottom pedestal of the triaxial apparatus.

### Horizontal Disk Transducers

The rubber membranes used for specimen preparation in the large triaxial apparatus are of thickness 2 mm. Initially, twelve numbers of 2 mm diameter holes were cautiously made in the membrane by a punching device. Aluminum plates of sizes 20×20×1 mm were pasted using silicone on the inside of the membrane to cover the holes. Utmost care should be taken so as to avoid leakage through the holes. The membrane was secured to the bottom pedestal by rubber straps, and cubical split mold was used to prepare specimens of size approximately 236×236×500 mm (Figure 7). Oiso gravels were pluviated inside the mold in ten layers, and each layer was compacted by giving 25 blows using a metallic rammer.



Figure 7 Rectangular mold for specimen preparation

After specimen preparation, on each face of the sample, one P- and two S- plates were glued by means of instant adhesive to the aluminum plates with a 1 mm thick acrylic disk in between (Figs. 8). This innovative arrangement of vertical and horizontal disk transducers (DTs) enables the measurement of nine different stiffnesses to describe the stiffness anisotropy (Fig. 9).

The notation of moduli of the form  $G_{xy}$  indicates shear modulus calculated from shear wave velocity propagating in the  $x$ -direction and oscillating in the  $y$ -direction. In the present contribution, the discussions will be made based on specimen prepared at a void ratio and relative density of 0.499 and 87%, respectively.

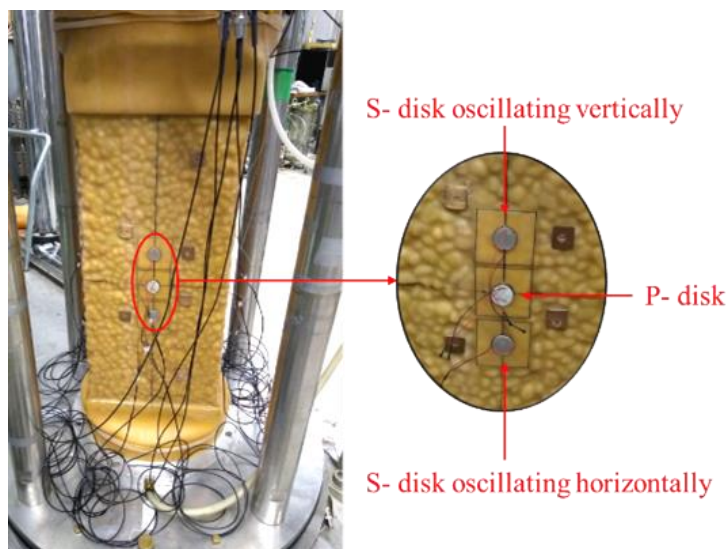
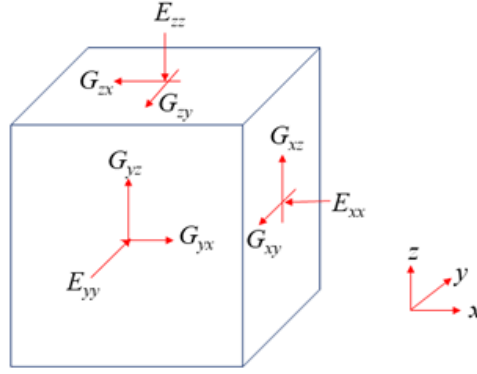


Figure 8 Specimen with horizontal disk transducers





**Figure 9** Notation of multidirectional stiffness

## DETERMINATION OF STIFFNESS

Peak-to-peak method was used to acquire  $V_s$  as rise signals are affected by near-field effect. The  $V_s$  evaluated from the peak-to-peak and rise-to-rise method were found to be comparable, when the excitation frequency coincides with one of the dominant frequencies (Dutta et al. (2019)). To measure  $V_p$ , rise-to-rise method as described in Dutta et al. (2019) was found to be appropriate.

The multidirectional small strain shear moduli were calculated using equation (1) from six different wave velocities, which were determined from the time domain responses displayed in Figures 10, 11, 12.

$$G_o = \rho V_s^2 \quad (1)$$

where,  $G_o$  is the small strain shear modulus,  $\rho$  is density of the specimen,  $V_s$  is shear wave velocity.

The multidirectional small strain Young's moduli were calculated using the equations (2) to (4).

$$M_o = \rho V_p^2 \quad (2)$$

where,  $M_o$  is the small strain constrained modulus,  $\rho$  is density of the specimen,  $V_s$  is compression wave velocity

$$E_o = \frac{M_o(1-2\nu)(1+\nu)}{(1-\nu)} \quad (3)$$

where,  $E_o$  is the small strain Young's modulus,  $\nu$  is the Poisson's ratio calculated using equation (4)

$$\nu = \frac{(V_p^2 - 2V_s^2)}{2(V_p^2 - V_s^2)} \quad (4)$$

The  $\nu$  used for the calculation of  $E_o$  (using equation 3) are the average of the two  $\nu$  values measured from equation 4 with  $V_s$  of two mutually perpendicular oscillation directions.

## RESULTS AND DISCUSSIONS

### *Multidirectional shear moduli*

The time domain responses for shear waves propagating in  $z$ - direction (vertically) and oscillating in  $x$ - and  $y$ - directions are given in Fig. 10 (a) and 10 (b) respectively. The first peak has been indicated by green arrows in the time domain plots. For  $V_{s(x)}$ , clear peaks can be identified for 2 kHz and 2.5 kHz input signals; but for frequencies exceeding 2.5 kHz, distorted output waveforms with no well-defined peaks are detected. However, for  $V_{s(y)}$ , distinct peaks can be visualized for all the excitation frequencies. It can be further noted that the travel time for  $V_{s(y)}$  waves are shorter than  $V_{s(x)}$  signals.

The time domain responses for shear waves propagating  $x$ - direction (horizontally) and oscillating in  $y$ - and  $z$ - directions are shown in Fig. 11 (a) and 11 (b) respectively. A quicker arrival of output response is observed for  $V_{s(xy)}$  waves as compared to  $V_{s(xz)}$ . Moreover, the amplitudes of output waveforms are considerably smaller for  $V_{s(xz)}$  responses as compared to  $V_{s(xy)}$  signals.

The time domain responses for shear waves propagating  $y$ - direction (horizontally) and oscillating in  $x$ - and  $z$ - directions are depicted in Fig. 12 (a) and 12 (b) respectively. A significantly faster arrival of output signal is detected for  $V_{s(yz)}$  waves as compared to  $V_{s(yx)}$ . A reduced output amplitude is noticed for  $V_{s(yx)}$  responses as compared to  $V_{s(yz)}$  signals. Furthermore, referring to Figure 11 (a) and Figure 12 (a), the arrival times of  $V_{s(xy)}$  and  $V_{s(yx)}$  are observed to be comparable.

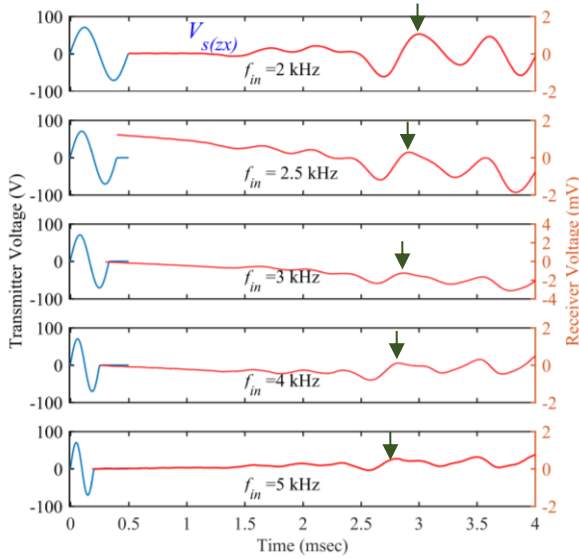


Fig. 10 (a) S- wave (Propagating in  $z$  direction and oscillating in  $x$  direction) ( $l_z=499.9$  mm,  $p'=50$  kPa &  $e_o=0.499$ )

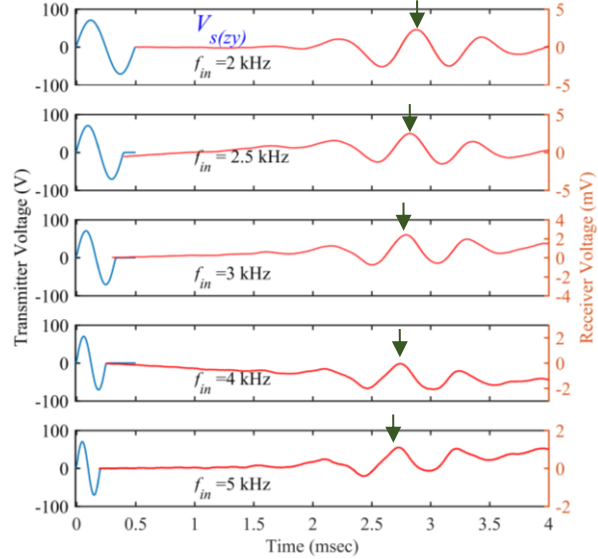


Fig. 10 (b) S- wave (Propagating in  $z$  direction and oscillating in  $y$  direction) ( $l_z=499.9$  mm,  $p'=50$  kPa &  $e_o=0.499$ )

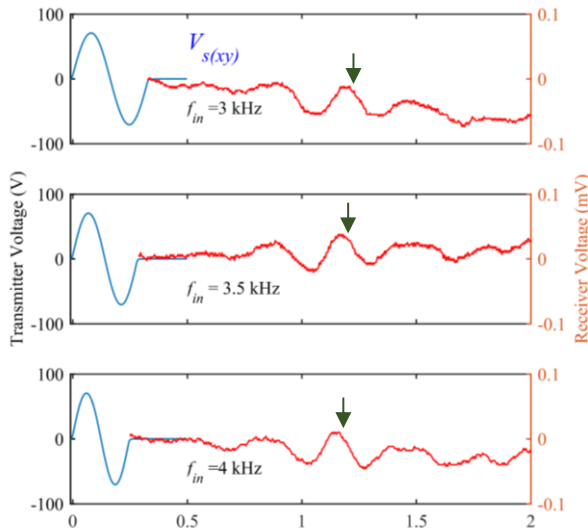


Fig. 11 (a) S- wave (Propagating in  $x$  direction and oscillating in  $y$  direction) ( $l_x=237.8$  mm,  $p'=50$  kPa &  $e_o=0.499$ )

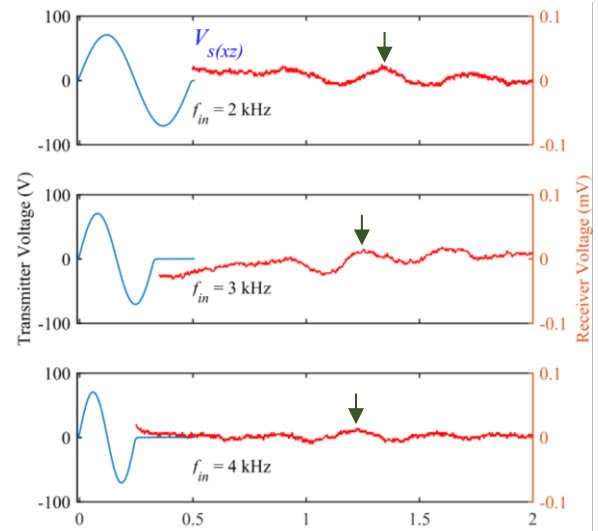


Fig. 11 (b) S- wave (Propagating in  $x$  direction and oscillating in  $z$  direction) ( $l_x=237.8$  mm,  $p'=50$  kPa &  $e_o=0.499$ )

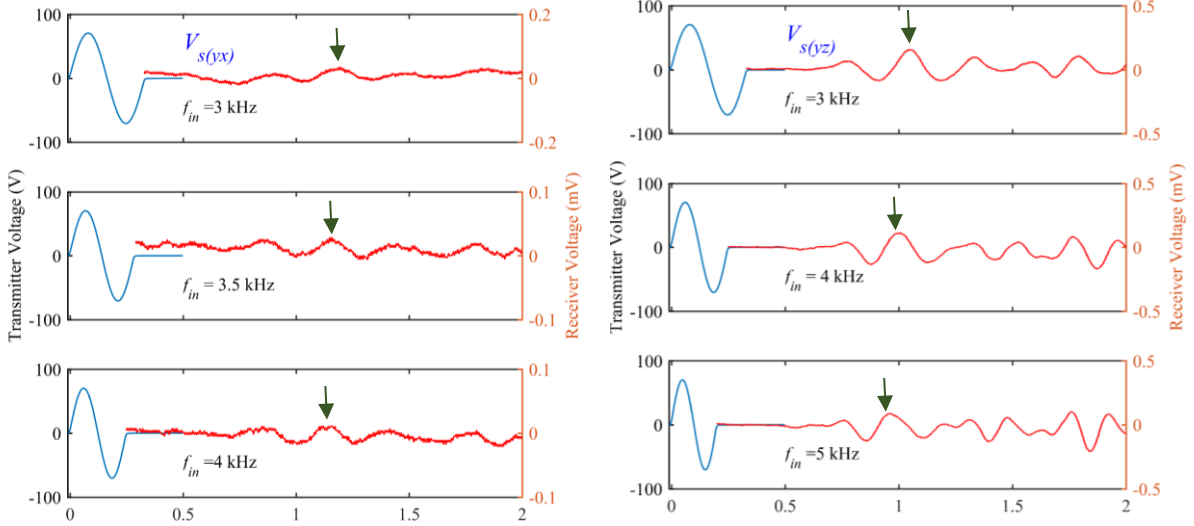


Fig. 12 (a) S- wave (Propagating in y direction and oscillating in x direction) ( $l_y=236.5$  mm,  $p'=50$  kPa &  $e_o=0.499$ )

Fig. 12 (b) S- wave (Propagating in y direction and oscillating in z direction) ( $l_y=236.5$  mm,  $p'=50$  kPa &  $e_o=0.499$ )

Figure 13 depicts six different multidirectional shear moduli for isotropic confining pressures of 30 and 50 kPa. The blue and red lines indicate moduli measured from waves propagating in vertical and horizontal directions, respectively. It can be noted that the order of shear moduli is  $G_{yz} > G_{xy} \approx G_{yx} > G_{xz} > G_{zy} > G_{zx}$ . The assumption of horizontal isotropy which is not exhibited by Oiso gravel may be ascribed to the large particle size.

For Oiso gravel, greater shear moduli have been obtained from both vertical and horizontal wave measurements in y direction as compared to x direction. Moreover,  $G_o$  quantified from waves propagating in horizontal directions are found to be higher than waves propagating in vertical direction. By performing wave velocity measurements using bender elements on sands and glass beads, similar observation has been reported by Kuwano (1999) and Kuwano & Jardine (2002).

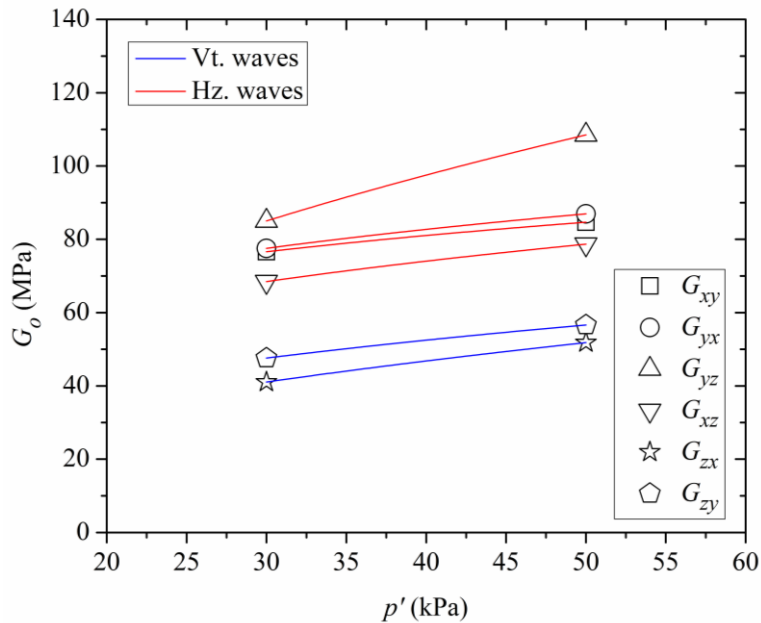


Fig. 13  $G_o$ -  $p'$  (Vt.- vertically propagating & Hz.- Horizontally propagating waves)

### Multidirectional Young's moduli

Figures 14 (a), (b) and (c) present the P- wave time domain responses of waves propagating in  $z$ ,  $x$  and  $y$  directions respectively. The rise points are shown by green arrows in the time domain plots. A relatively shorter compression wave travel time can be noted in  $y$  direction as compared to  $x$  direction, signifying a stiffer response in  $y$  direction, which is consistent with the S- wave measurements.

Figure 15 portrays three different multidirectional Young's moduli for isotropic confining pressures of 30 and 50 kPa. The blue and red lines signify moduli determined from waves traversing in vertical and horizontal directions, respectively. It can be perceived that the order of Young's moduli is  $E_{yy} > E_{xx} > E_{zz}$ . A significantly larger Young's moduli are recorded in  $y$  direction as compared to  $z$  direction. At an isotropic confining pressure of 50 kPa, the ratio of  $E_{yy}$  to  $E_{zz}$  is observed to be as high as 1.75.

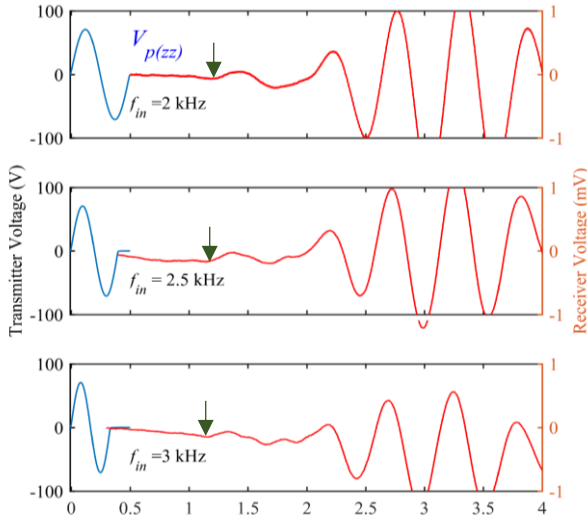


Fig. 14 (a) P- wave (Propagating in  $z$  direction) ( $l_z=499.9$  mm,  $p'=50$  kPa &  $e_o=0.499$ )

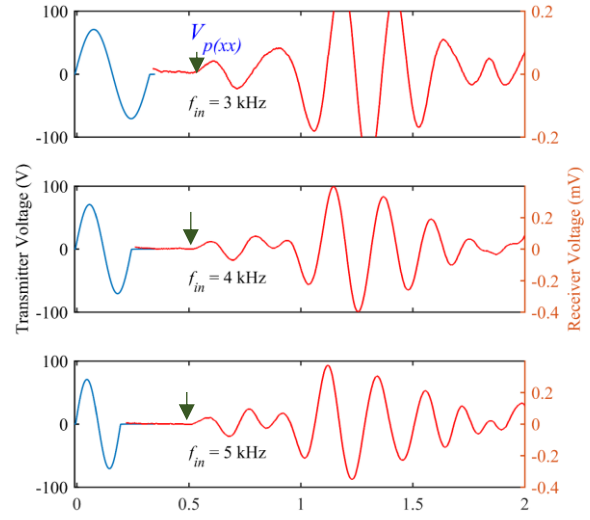


Fig. 14 (b) P- wave (Propagating in  $x$  direction) ( $l_x=237.8$  mm,  $p'=50$  kPa &  $e_o=0.499$ )

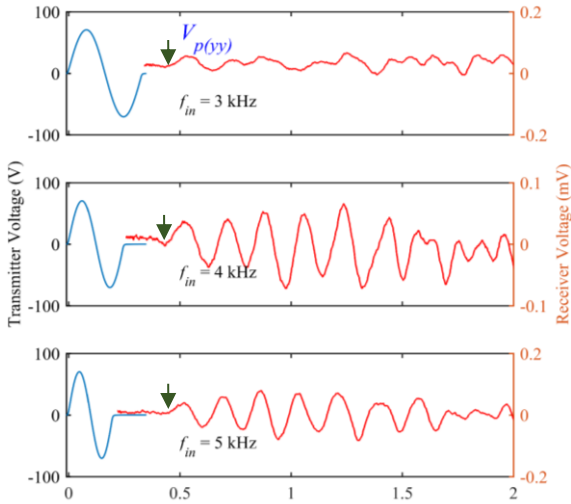


Fig. 14 (c) P- wave (Propagating in  $y$  direction) ( $l_y=236.5$  mm,  $p'=50$  kPa &  $e_o=0.499$ )

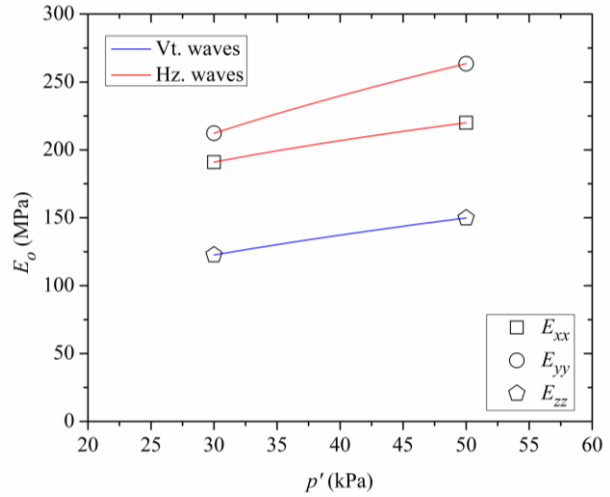


Fig. 15  $E_o$ -  $p'$  (Vt.- vertically propagating & Hz.- Horizontally propagating waves)



## CONCLUSIONS

In the current contribution, an innovative design of vertical and horizontal disk transducers was described which can estimate nine different small strain moduli to complete the stiffness matrix. To display the suitability of the apparatus to test a wide range of particle sizes, S- and P- wave measurements were performed on a uniformly graded Oiso gravel of median particle size 11.8 mm. For Oiso gravel, the small strain shear and Young's moduli measured in horizontal direction are considerably greater than those measured in vertical direction. Moreover, the approximation of horizontally isotropic behavior is found to be not valid for Oiso gravel.

## REFERENCES

- AnhDan, L., Koseki, J., Sato, T. (2002) Comparison of Young's moduli of dense sand and gravel measured by dynamic and static methods. *Geotechnical Testing Journal*, 25(4), 349-368.
- Brignoli, E., Gotti, M., & Stokoe, K. (1996) Measurement of shear waves in laboratory specimens by means of piezoelectric transducers. *Geotechnical Testing Journal*, 19 (4), 384-397.
- Dutta, T. T., Otsubo, M., Kuwano, R., & Sato, T., Development of vertical and horizontal disk transducers for wave velocity measurements in a large rectangular specimen, 7th International Symposium on the Deformation Characteristics of Geomaterials, Glasgow, U.K., 26-28th June 2019.
- Dutta, T. T., Otsubo, M., Kuwano, R., & O'Sullivan, C. (2019) Apparent particle size dependency and appropriate excitation frequency range for wave velocity estimation in granular materials. *Géotechnique Letters* (under review)
- Escribano, D.E. & Nash, D.F.T. (2015) Changing anisotropy of  $G_o$  in Hostun sand during drained monotonic and cyclic loading. *Soils and Foundations*, 55 (5), 974-984.
- Hoque, E., and Tatsuoka, F. (1998) Anisotropy in elastic deformation of granular materials. *Soils and Foundations*, 38(1), 163–179.
- Ismail, M.A., & Rammah, K.I. (2005) Shear-plate transducers as a possible alternative to bender elements for measuring  $G_{max}$ . *Géotechnique*, 55 (5), 403-407.
- Jiang, G.-L., Tatsuoka, F., Flora, A., and Koseki, J. (1997) Inherent and stress state induced anisotropy in very small strain stiffness of a sandy gravel. *Geotechnique*, 47 (3), 509–521.
- Kokusho, T. and Yoshida, Y. (1997). SPT N-value and S-wave velocity for gravely soils with different grain size distribution. *Soils and Foundations*, 37 (4), 105–113.
- Kuwano, R. (1999) The stiffness and yielding anisotropy of sand. PhD thesis, Imperial College London.
- Kuwano, R & Jardine, R.J. (2002) On the applicability of cross-anisotropic elasticity to granular materials at very small strains. *Géotechnique*, 52(10), 727-750.
- Lawrence, F. V. (1963). Propagation of ultrasonic waves through sand. Research Report R63-08, Massachusetts Institute of Technology, Boston.
- Modoni, G., Flora, A., Mancuso, C., Viggiani, C., and Tatsuoka, F. (2000) Evaluation of gravel stiffness by pulse wave transmission tests *Geotechnical Testing Journal*, Vol. 23 (4), 506–521.
- Ng, C. W. W. & Yung, S. Y. (2008) Determination of the anisotropic shear stiffness of an unsaturated decomposed soil. *Géotechnique*, 58 (1), 23–35
- Pennington, D. S., Nash, D. F. T., and Lings, M. L. (1997) Anisotropy of  $G_0$  Shear Stiffness in Gault Clay. *Géotechnique*, 47 (3), 391–398.
- Santamarina, J. C. & Cho, G. C. (2004) Soil behaviour: the role of particle shape. *Advances in Geotechnical Engineering: The Skempton Conference*, pp. 604–617. London: Thomas Telford.
- Shirley, D.J., & Hampton, L.D. (1978) Shear-wave measurements in laboratory sediments. *Journal of Acoustical Society of America*, 63 (2), 607-613.
- Suwal, L.P., & Kuwano, R. (2013) Disk shaped piezo-ceramic transducer for P and S wave measurement in a laboratory soil specimen. *Soils and Foundations*, 53 (4), 510–524.
- Wang, Y.H. and Mok, C.M.B. (2008) Mechanisms of small-strain shear-modulus anisotropy in soils. *Journal of Geotechnical and Geoenvironmental Engineering*, 134 (10), 1516-1530.